

OPEN ACCESS

Stave module design and development of the new ALICE Inner Tracking System

To cite this article: W. Poonsawat *et al* 2019 *JINST* **14** P05003

View the [article online](#) for updates and enhancements.



IOP | ebooks™

Bringing you innovative digital publishing with leading voices to create your essential collection of books in STEM research.

Start exploring the collection - download the first chapter of every title for free.

Stave module design and development of the new ALICE Inner Tracking System

W. Poonsawat,^{a,c,1} C. Kobdaj,^{a,c} M. Sitta^{b,c} and Y. Yan^{a,c,1} on behalf of ALICE ITS collaboration

^a*School of Physics, Institute of Science, Suranaree University of Technology, Nakhon Ratchasima 30000, Thailand*

^b*Dipartimento di Scienze e Innovazione Tecnologica, Università Piemonte Orientale, Viale T. Michel 11, Alessandria, Italy*

^c*CERN, Geneva, CH-1211 Switzerland*

E-mail: wanchaloem.poonsawat@cern.ch, yupeng@sut.ac.th

ABSTRACT: The aim of the ALICE Collaboration is to study the physics of strongly interacting matter by using the experimental results from a dedicated heavy-ion detector. The Inner Tracking System (ITS) is located at the heart of the ALICE detector surrounding the interaction point. Currently, ALICE is planning to upgrade the ITS for rare probes at low transverse momenta. The new ITS comprises seven layers of silicon pixel sensors on the supporting structure. One goal of the new design is to reduce the material budget (X/X_0) per layer to 0.3% for the inner layers and 0.8% for the middle and outer layers. In this work, we perform simulations based on detailed geometrical descriptions of different supporting structures for the inner and outer barrels by using ALIROOT.² Our results indicate that it is possible to reduce the material budget of the inner and outer barrels to the expected value. Manufacturing of such prototypes is also possible.

KEYWORDS: Detector design and construction technologies and materials; Detector modelling and simulations I (interaction of radiation with matter, interaction of photons with matter, interaction of hadrons with matter, etc); Particle tracking detectors (Solid-state detectors)

¹Corresponding author.

²ALICE Off-line framework operated on ROOT system. This is a fundamental framework used for simulation, reconstruction and analysis.

Contents

1	Introduction	1
2	Current and upgraded Inner Tracking System	1
3	Stave design for ITS upgrade	3
4	Toward the material budget (X/X_0) reduction of the inner barrel	4
5	Outer barrel stave	5
6	Conclusions	8

1 Introduction

A Large Ion Collider Experiment (ALICE) is designed to study the properties of quark-gluon plasma, a deconfined state of strongly interacting matter. There are eighteen systems within the ALICE detector, but in this work, we are interested in the central part of the ALICE detector called the Inner Tracking System (ITS). The present ITS is composed of six layers exploiting three different silicon technologies. The main purpose of the ITS is to detect the primary (collision location) and secondary vertices (decay location of some unstable heavy particles after a flight distance of some hundreds of micrometers). The innermost layers are required to be high-resolution devices to record with the highest precision the coordinates of the points crossed by each passing particle [1].

The precision of the present ITS for detecting charm mesons is insufficient at low transverse momenta ($< 1 \text{ GeV}/c$) and even worse for charm baryons. In the case of a charm baryon, the lowest-mass charm baryon is Λ_c with a rest mass of $2286.46 \pm 0.14 \text{ MeV}/c^2$ [2]. The important channel of its measurement is the decay of $\Lambda_c \rightarrow pK^-\pi^+$ with a branching ratio equal to $5.0 \pm 1.3\%$. The mean proper decay length ($c\tau$) of Λ_c is only $60 \mu\text{m}$ that is shorter than the impact parameter resolution of the present ITS. Therefore, charm baryons are only partially accessible by the ALICE detector in central Pb-Pb collisions.

Current measurements of Pb-Pb collisions are characterized by a very small signal-over-background ratio, which requires large statistics. Thus, to reach the goal of heavy quark measurement, the ALICE ITS must be upgraded [3].

2 Current and upgraded Inner Tracking System

The current ITS features three different types of silicon tracking detectors. Silicon pixel detectors are used in the first two innermost layers. The next two layers are composed of silicon drift detectors, and the two outermost layers are equipped with silicon strip detectors [3].

Reduction in the upgraded beam-pipe radius from 2.94 to 1.98 cm allows us to place the innermost layer 9.6-mm closer to the interaction point. An additional layer is also introduced to increase the tracking efficiency of the new ITS. This new design is expected to improve the impact parameter resolution by a factor of three [3]. The use of monolithic active pixel sensors for the seven layers of the upgraded ITS can reduce the material budget by a factor of 7 (50 μm of silicon is used instead of 350 μm) per layer [4]. For data readout, a new front-end timing and data transfer architecture will be developed to increase the readout frequency up to 50 MHz for Pb-Pb interaction and about 200 kHz for pp interactions [5]. The new cooling system is also improved to ensure a better heat transfer.

The design of the new ITS is composed of the inner barrels (layers 0 to 2), middle barrels (layers 3 to 4), and outer barrels (layers 5 to 6) (see figure 1).

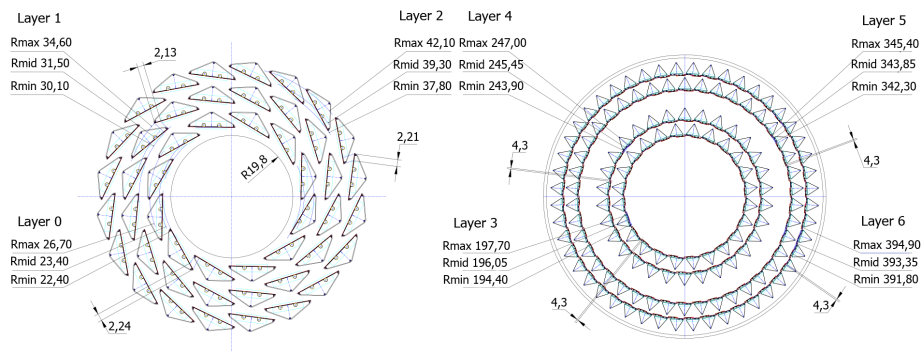


Figure 1. Cross-section view of the Inner Barrel (left) and Outer Barrel (right) [6]. Reproduced from [6]. © IOP Publishing Ltd. All rights reserved.

The expected material budget of the new design has been calculated by summing the overall material budget of each detector component without considering the detailed geometry. The design goal of the supporting structure and material budget of the new layout are given in table 1.

Table 1. Layout of the upgrade scenario for the ITS inner barrel. The numbers in brackets refer to the case of the current detector.

Layer	Radius (cm)	Material budget ($\%X_0$)
<i>inner barrel</i>		
1 pixel (pixel)	2.2 (3.9)	0.3 (1.14)
2 pixel (pixel)	2.8 (7.6)	0.3 (1.14)
3 pixel (none)	3.6 (-)	0.3 (-)
<i>mid barrel</i>		
4 pixel (drift)	20.0 (15.0)	0.8 (1.13)
5 pixel (drift)	22.0 (23.9)	0.8 (1.26)
<i>outer barrel</i>		
6 pixel (strip)	41.0 (38.0)	0.8 (0.83)
7 pixel (strip)	43.0 (43.0)	0.8 (0.83)

3 Stave design for ITS upgrade

The upgraded ITS layers, both the inner and the outer barrels, are composed of the particle tracking module named *stave*. Stave is a composite element devised to be a support structure. It consists of a space frame, cold plate, and hybrid integrated circuit.

In this work, different stave designs have been studied for their material budget. The space frame of each stave design is made of light filament-wound carbon fibers. It is obtained by winding a high modulus carbon fiber rowing with respect to the stave long axis with an angle of 45° . The winding angle and number of helices have been optimized to achieve the best compromise between material budget and stiffness.

For the cooling system, a cold plate is used to remove the heat dissipated from the pixel chips. The cold plate is made of a high thermally conductive carbon fiber laminate, on top of which the silicon chips are glued. The heat is conducted into the cooling pipes or microchannel embedded in the cold plate and is removed by the coolant. In order to achieve the lowest material budget, the cold plates of the stave have been considered in four different models for the various geometrical designs.

The mechanical support structure is designed under technical constraints such as the detector layout, specific sensor chip size, and cooling technology requirements. The stave structures have been classified into the following models:

- (i) *Model 0-Wound truss structure with cooling pipes at the vertices*: winding carbon filaments with a diameter of 5 mm are used to construct the support structure. High thermal conductivity carbon fibers are used for the two embedded pipes. The pyramidal structure made of the carbon fiber filaments with two cooling pipes at the edge will be sufficiently strong to support the detection layer structure but insufficient to conduct the generated heat.
- (ii) *Model 1-Wound truss structure with polyimide microchannel cooling*: for this model, the cooling pipes are replaced by a cold plate for better heat distribution over the pixel chip. A monophasic or biphasic refrigerant fluid is used in the cold plate flowing into 0.16 mm^2 of the polyimide microchannel cooling section.
- (iii) *Model 2-Wound truss structure with a uniform carbon plate and polyimide tubes in the middle*: this model uses a uniform carbon plate for transferring heat to two embedded tubes. These polyimide tubes are placed in the middle at the base of the stave structure. However, the addition of a carbon plate may cause an increase in the amount of material.
 In this model, two different outer radii, 0.15 (*Model 2.1*) and 0.10 (*Model 2.2*) mm, of the cooling pipes are separately simulated for the material properties.
- (iv) *Model 3-Wound truss structure with silicon microchannel*: this model comprises the wound truss structure with the cold plate, made of a silicon substrate. Based on etching technology, the microchannel can be formed on the silicon plate inside which the cooling fluid flows.

By incorporating a detailed geometrical description of all models in ALIROOT, the material budget for all stave models can be completely calculated.

4 Toward the material budget (X/X_0) reduction of the inner barrel

The material budget of each stave prototype can be calculated from the radiation length of their components. It depends on either the thickness (X/X_0) or percentage of the covered surface ($X/X_0(\%)$) [7]. The material budget in ALIROOT is computed using fake particles, called “geantinos”. They can be shot straight toward the sensors, and because they have no charge, they suffer neither deviation nor any kind of energy loss. They are tracked as all other particles in each step. The user can restrict the volume crossed by geantinos by setting the minimum radius R_{\min} and maximum radius R_{\max} , the minimum and maximum ϕ values, and the range along the longitudinal axis Z , between $-Z_{\min}$ and $+Z_{\max}$, of the traveling region. The material budget can be determined in essentially two ways. In the first approach, the geantino tracks are generated perpendicular to the longitudinal axis of the staves; hence, the actual material budget can be determined. In the second method, all geantinos originate from the interaction point, so the computed material budget is the same as seen by real particles originating from the collisions.

The stave design accounts for the material budget requirement, which is limited to 0.3% for the inner barrel and 0.8% for the outer barrel [3]. The simulations include essentially all material properties used in each model, as shown in table 2 and table 3.

Table 2. List of the stave components and their thicknesses used in ALIROOT simulation. The numbers in brackets refer to the parameters used in the ALICE ITS conceptual design report [3].

Material	Model 0	Model 1	Model 2.1	Model 2.2	Model 3	Model 4
Thickness [μm]						
Filament						
Top CFRP M60J 3K	70 (70)	200 (120)	200 (100)	200 (100)	200 (120)	200 (100)
Bottom CFRP M60J 3K	70 (-)	200 (240)	—	—	200 (240)	—
Cooling						
Pipe Kapton	70 (70)	—	130 (70)	130 (70)	—	130 (70)
water	1450 (1450)	—	1450 (1450)	940 (940)	—	940 (940)
Carbon plate	—	—	140 (140)	140 (140)	—	140 (140)
Sensor						
Glue	125 (200)	250 (200)	100 (200)	100 (200)	250 (200)	100 (200)
Silicon chip			50 (50)			
Flex cable			100 (-)			
Polyimide Microchannel	—	100 (100)	—	—	—	—
Silicon Microchannel	—	—	—	—	40 (40)	—
water	—	200 (200)	—	—	160 (160)	—

The calculated results for the material budget of different models of the inner barrel are presented in figure 2. In both approaches, the material budget has been computed in terms of the average material budget contribution. The highest peaks represent the overlap between each stave. In model 2.2, the location of the cooling pipes around the middle of the stave can help to enhance the thermal conductivity despite the higher material budget than model 0. The second highest peaks in figure 2(c) and figure 2(d) are due to the polyimide cooling pipes filled with water. Instead of cooling pipes, using microchannel-filled water in model 1 or Freon in model 3 as a coolant can serve

Table 3. List of the stave components and their contribution to the radiation length. The numbers in brackets refer to the approximation value used in CDR [3, 8, 8, 10].

Material	Model 0	Model 1	Model 2.1	Model 2.2	Model 3	Model 4
	X_0 [cm]					
Filament						
Top CFRP M60J 3K				19 (25)		
Bottom CFRP M60J 3K	19 (25)	19 (25)	—	—	19 (25)	—
Cooling						
Pipe Kapton	28.4 (28.6)	—	28.4 (28.6)	28.4 (28.6)	—	28.4 (28.6)
water	35.8 (36.1)	—	35.8 (36.1)	35.8 (36.1)	—	35.8 (36.1)
Amec Thermasol FGS 003	—	—	27 (25)	27 (25)	—	27 (25)
C Fleece	—	—	106 (25)	106 (25)	—	106 (25)
Sensor						
Glue				44.37 (44.4)		
Silicon chip				9.35 (9.36)		
Flex cable				13.3 (13.3)		
Polyimide Microchannel	—	28.4 (28.6)	—	—	—	—
Silicon Microchannel	—	—	—	—	9.35 (9.36)	—
water	—	35.8 (36.1)	—	—	35.8 (36.1)	—
K13D2U 2K	—	—	26 (25)	26 (25)	—	26 (25)
C Fleece	—	—	106 (25)	106 (25)	—	106 (25)

as a better method to dissipate the heat from the sensors [5]. The results show that all simulated and calculated material budget agree with a certain underestimation for the calculated values. The material budget calculations for all stave prototypes is summarized in table 4.

Table 4. Overall material budget obtained from ALIROOT simulation for different stave prototypes compared to the theoretical calculation in CDR [3]. Model 2.2 is suggested to reduce the large material budget contribution of the cooling pipe obtained from the completed simulation with the fully detailed geometry.

Stave prototype	X/X_0 [CDR] (%)	X/X_0 [ALIROOT] (%)
Model 0	0.26	0.284
Model 1	0.30	0.334
Model 2.1	0.31	0.344
Model 2.2	0.30	0.303
Model 3	0.25	0.249

5 Outer barrel stave

The conceptual design of the outer barrel stave is similar to that of the inner barrel. However, the bottom of the supporting part is split longitudinally into two half-staves in the azimuthal direction, i.e., along with the phi angle, as shown in figure 3. Each half-stave consists of seven sensor chips

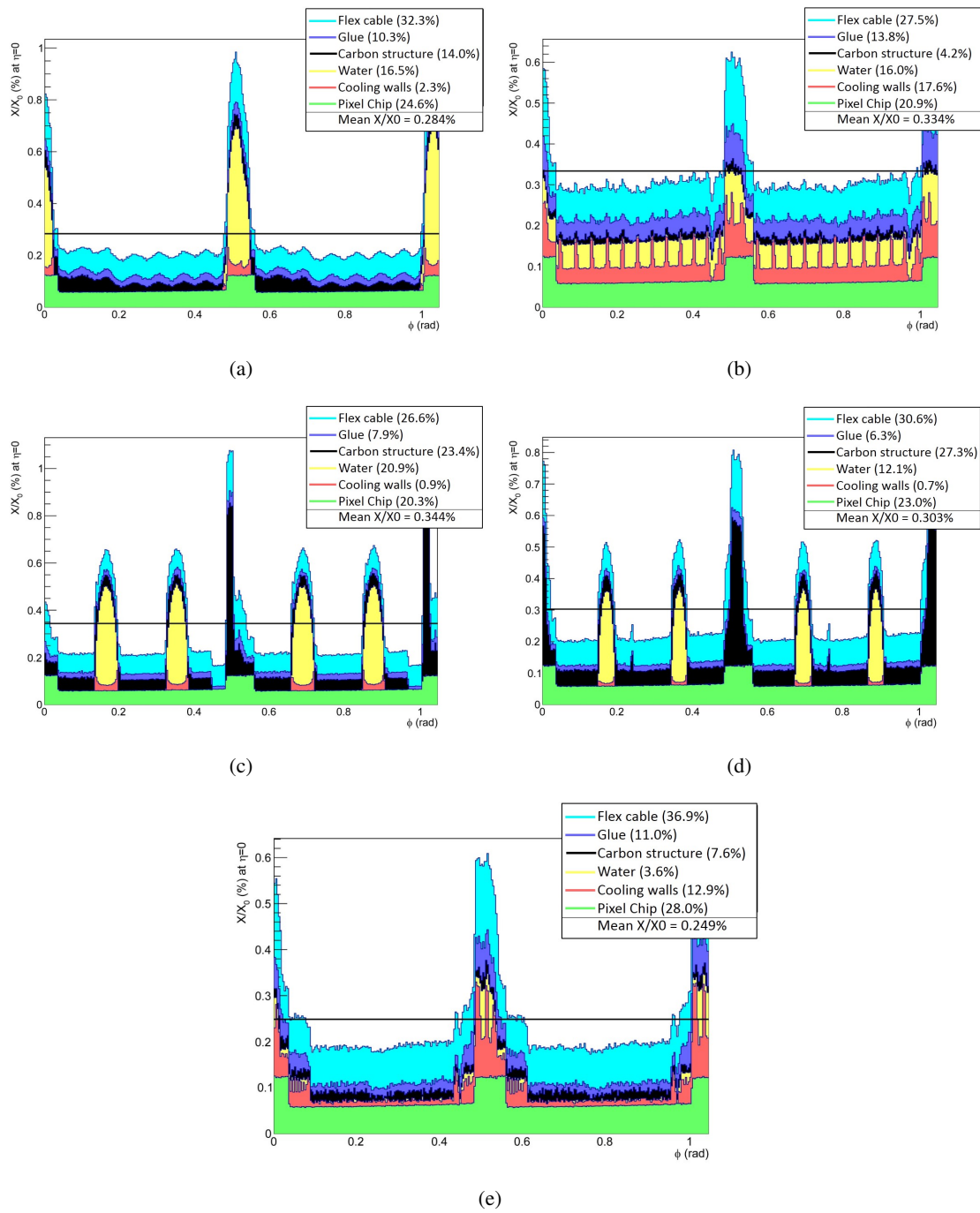


Figure 2. Material budget distribution of (a) model 0, (b) model 1, (c) model 2.1, (d) model 2.2, and (e) model 3. Each figure shows the contribution of two staves depending on the stave width coverage and the average material budget calculated per stave. The x-axis is the simulation range of the stave width. The highest peak of each model arises from the overlap at the edges of the carbon structure, while the smaller peaks around 0.5% X_0 in model 2.1 and 2.2 correspond to the polyimide cooling pipes filled with water. The major contribution of the material budget originates from the flex cable.

with integrated cooling pipes and cold plates. These two pipes have an inner diameter of 2.67 mm and are filled with water.

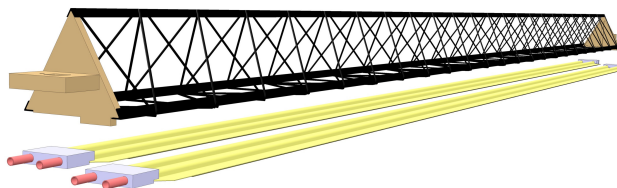


Figure 3. Schematic of the layout of the mechanical and cooling structure of the outer barrel stave [6]. Reproduced from [6]. © IOP Publishing Ltd. All rights reserved.

The staves of the outer barrels have been designed to achieve the required stiffness and thermal properties as expected in the inner barrels. Several components, similar to the inner barrel, are used to prototype the outer barrel stave with seven pixel chips. The estimates of the contribution of the outer barrel stave to the material budget are reported in table 5.

Table 5. List of the outer stave components and their thickness and the estimated contributions to the material budget [6].

Stave element	Component	Material	Thickness [μm]	X/X_0 [cm]	X/X_0 [%]
Module	FPC Metal layers	Aluminum	50	8.896	0.056
	FPC Insulating layers	Polyimide	100	28.41	0.035
	FPC Insulating layers	Polyimide	100	28.41	0.035
	Module plate	Carbon fiber	120	26.08	0.046
	Pixel Chip	Silicon	50	9.369	0.053
	Glue	Eccobond 45	100	44.37	0.023
Power Bus	Metal layers	Aluminum	200	8.896	0.225
	Insulating layers	Polyimide	200	28.41	0.070
	Glue	Eccobond 45	100	44.37	0.023
Cold Plate		Carbon fleece	40	106.80	0.004
		Carbon paper	30	26.56	0.011
	Cooling tube wall	Polyimide	64	28.41	0.013
	Cooling fluid	water		35.76	0.105
	Carbon plate	Carbon fiber	120	26.08	0.046
	Glue	Eccobond 45	100	44.37	0.023
	Space Frame		Carbon rowing		
Total					0.813

The results of the simulation of the material distribution across the outer barrel staves are presented in figure 4. The half-staves are partially superimposed surrounding the detector, thus giving rise to the peaks at about 1.25% X/X_0 . The highest peaks are due to the polyimide cooling pipes, filled with water, embedded in the cold plate. Splitting the support structure results in the larger contribution of the flex cable than for the inner barrel because the increased number of chips

and the associated electric circuit require more stiffness. The estimated overall material budget is within the expected 0.8% X/X_0 .

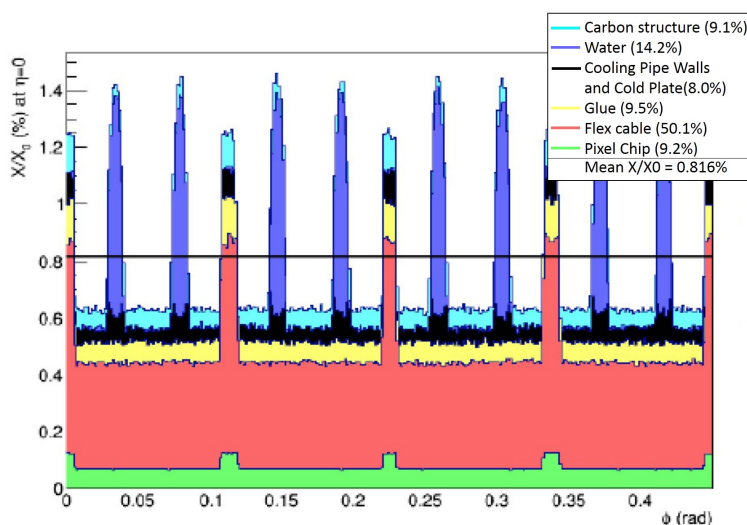


Figure 4. Material budget distribution of outer barrel prototype. The highest peaks correspond to the polyimide cooling pipes filled with water embedded in the cold plate. The other peak represents the half-stave overlaps. The high contribution of flex cable is due to the thick copper layers [6]. Reproduced from [6]. © IOP Publishing Ltd. All rights reserved.

6 Conclusions

The upgrade to the ITS design is aimed at improving the impact parameter resolution and tracking efficiency of the ALICE detector and reducing the statistical uncertainty for low transverse momentum scattering. The construction of stave prototypes and the application of a new cooling system will achieve a reduction in the material budget for the new ITS. Presently, the ALIROOT simulation shows encouraging results for the estimation of the material budget. For the inner barrel, the results show that the use of lightweight carbon structure with polyimide cooling pipes can reduce the material budget to 0.3% per layer for model 2. The addition of an innermost layer and the use of smaller pixel size CMOS sensors can extend the coverage radius and perform the coverage pseudo-rapidity ($|\eta| \leq 1.22$). Adding a detection layer also provides continuous coverage for charged particle multiplicity measurement. The simulation performed thus far guarantees that the conceptual design used in the new ITS satisfies the requirements of the upgraded ALICE detector.

Finally, model 2 is chosen for the final production of the upgrade ITS. Although model 2's material budget is not the lowest, it provides the optimal production cost and better thermal conductivity than models 0, 1, and 3. Model 3 improves upon model 1 by trying to reduce the size of the cold plate. However, the thinner polyimide cold plate could provide more opportunities for water to leak, which is why the design team proposed the silicon microchannel instead of polyimide. However, this material selection leads to other problems, i.e., technical difficulties and a high production cost. Thus, the appropriate model for the inner barrel stave structure is the revised model 2.2, now called model 4. Stave production is currently ongoing for the structural characterization and the final assembly of the detector module [6].

Acknowledgments

We would like to thank L. Musa and also the ALICE ITS upgrade team for their assistance at CERN. This work was supported by the Suranaree University of Technology (SUT) and by the Office of the Higher Education Commission under the NRU project of Thailand (SUT-PhD/07/2556). CK and YY acknowledge support from the SUT and CHE-RNU project (SUT-COE: High Energy Physics & Astrophysics).

References

- [1] L. Evans, *The Large Hadron Collider: A Marvel of Technology*, EPFL Press, (2009).
- [2] PARTICLE DATA GROUP collaboration, *Review of particle physics*, *J. Phys. G* **37** (2010) 075021.
- [3] ALICE collaboration, *Conceptual Design Report for the Upgrade of the ALICE ITS*, [CERN-LHCC-2012-005](#) [LHCC-G-159].
- [4] R. Lemmon, *The ALICE Inner Tracking System Upgrade*, *Nucl. Phys. A* **904** (2013) 937C.
- [5] ALICE ITS collaboration, *Upgrade of the ALICE Inner Tracking System*, *Nucl. Instrum. Meth. A* **731** (2013) 40 [[arXiv:1211.5216](#)].
- [6] ALICE collaboration, *Technical Design Report for the Upgrade of the ALICE Inner Tracking System*, *J. Phys. G* **41** (2014) 087002 [CERN-LHCC-2013-024] [ALICE-TDR-017].
- [7] S. Tavernier, *Interactions of Particles in Matter*, Springer, (2010).
- [8] C. Gargiuloetal, *Studies on the composite light structure for the ALICE Silicon tracker upgrade*, talk given at *Forum on tracker detectors mechanics*, CERN, Geneva, Switzerland, July 2012.
- [9] M. Gupta, *Calculation of radiation length in materials*, PH-EP-Tech-Note-2010-013 (2010).
- [10] PARTICLE DATA GROUP collaboration, *Review of Particle Physics*, *Phys. Rev. D* **98** (2018) 030001.